Plasma Phys. Control. Fusion **53** (2011) 035005 (9pp) doi:10.1088/0741-3335/53/3/035005

Soft x-ray measurements of resistive wall mode behavior in NSTX*

L Delgado-Aparicio[1,5], D Stutman[2], S A Sabbagh[3], R E Bell[1], J W Berkery[3], K Tritz[2], S P Gerhardt[1], B LeBlanc[1], M Finkenthal[2], J P Levesque[3], K C Lee[4], J Menard[1], S Paul[1] and L Roquemore[1]

[1] Princeton Plasma Physics Laboratory, Princeton, NJ 08543, USA
[2] The Johns Hopkins University, Baltimore, MD 21218, USA
[3] Columbia University, New York, NY 10027, USA
[4] University of California at Davis, Davis, CA 95616, USA

E-mail: ldelgado@pppl.gov

Received 17 May 2010, in final form 2 December 2010
Published 27 January 2011
Online at stacks.iop.org/PPCF/53/035005

Abstract

A multi-energy soft x-ray (ME-SXR) array is used for the characterization of resistive wall modes (RWMs) in the National Spherical Torus Experiment (NSTX). Modulations in the time history of the ME-SXR emissivity profiles indicate the existence of edge density and core temperature fluctuations in good agreement with the slow evolution of the $n = 1$ magnetic perturbation measured by the poloidal and radial RWM coils. The characteristic 20–25 Hz frequency in the SXR diagnostics is approximately that of the $n = 1$ stable RWM, which is also near the measured peak of the resonant field amplification (RFA) and inversely proportional to the wall time. Together with the magnetics, the ME-SXR measurements suggest that in NSTX the RWM is not restricted exclusively to the reactor wall and edge, and that acting with the stabilizing coils on its global structure may result in density and temperature fluctuations that can be taken into account when designing the feedback process.

(Some figures in this article are in colour only in the electronic version)

1. Motivation

Stable plasma operation at high plasma pressure is the key for the realization of a compact and economical fusion reactor. One of the limiting factors for achieving such a condition is the pressure-driven resistive wall mode (RWM) [1–6] which is a branch of the magnetohydrodynamic (MHD) kink instability that can grow unstable on the slow eddy-current decay time of the resistive wall of the device, τ_w. The passive or active stabilization of this

* This paper was originally submitted as part of the special issue on MHD stability control in toroidal devices, see *Plasma Phys. Control. Fusion* 2010 **52** 100301–104006.
[5] On assignment at the Massachusetts Institute of Technology-Plasma Science Fusion Center.

long-wavelength instability is thus expected to significantly improve the performance of future burning plasma experiments. While in conventional high aspect-ratio low-β tokamaks the RWM has been studied and controlled for over a decade [2], in a high plasma pressure and low magnetic field device such as the high-β spherical tokamak (ST), the mitigation, control and understanding of the RWM become even more important [3–6]. We present here a study, which contributes to understanding the physics of RWM stabilization and control, based on the use of a 'multi-energy' soft x-ray (ME-SXR) array operated on the National Spherical Torus Experiment (NSTX) [7]. In section 2 of this paper we describe briefly the RWM experiments performed in NSTX H-mode plasmas as well as the ME-SXR diagnostic system used for the internal characterization of RWMs; the modulated localized SXR emissivities that will be identified as density and temperature fluctuations during the stable RWMs and the pressure-driven β_N-collapse associated also with RWMs will be pointed out in section 3. The conclusions and future work are included in sections 4 and 5, respectively.

2. RWM plasmas and ME-SXR internal diagnostics

2.1. H-mode features

RWM active stabilization has been successfully tested in NSTX [3–6]. The plasmas used were typical double-null-diverted (slightly shifted to lower single-null) NSTX H-modes having: $I_p = 0.9$ MA, $B_{\phi 0} = 0.45$ T, $\langle\kappa\rangle \sim 2.3$ and $\langle\delta\rangle \sim 0.6$ (see figure 1 and [5, 6]). The deuterium neutral beam injection had accelerating voltages of 90–95 kV and a total heating power of $P_{NBI} \sim 6.3$ MW with neutron rates of the order of $\sim 3.5 \times 10^{14}$ n s^{-1} (see figure 1(c)). The dc $n = 3$ magnetic braking field and the $n = 1$ active feedback were turned on simultaneously at approximately 0.45 s; the effect of the $n = 3$ magnetic braking field was to reduce the plasma toroidal rotation (and thus its passive stabilizing effect) triggering the RWM, while a superimposed $n = 1$ feedback field actively stabilized the RWM for several energy confinement times [5, 6]. These H-modes did not experience an unstable RWM and continued to increase their β_N from ~4.0 to 5.5 as the toroidal rotation continued to decrease throughout the major radius (see figure 1(b)). The data depicted in figures 1(c) and (d) show the low frequency ~20–25 Hz features (see black arrows) that will be associated throughout this paper with the $n = 1$ actively stabilized RWM [8, 9]. The D_α signals suggest the presence of an edge activity during active stabilization that correlates well in time with the signatures from the core neutron data; in addition, measurements obtained with a tangential bolometer also indicate transient increases in the total radiated power. A discrete inboard channel (Ch_1 ($R_{tg} \sim 32$ cm)) from the multichannel Far-infrared Tangential Interferometer/Polarimeter (FIReTIP) [15] also provides a measurement of the ~20–25 Hz electron density modulation during the active stabilization of the RWM (see figure 1(e)). This line-integrated density oscillation ($\tilde{n}_e/n_e \sim 2.5\%$) present during the RWM active stabilization appears to be dominant at the inboard (high-field side) edge, as suggested initially by the D_α measurement. The goal of this paper is to depict the existent correlation between the signatures measured by the wall RWM magnetic sensors shown in figure 1(f), the modulations of D_α, core beam-plasma neutron rate and volume averaged radiated power, with internal measurements of edge and core density and temperature fluctuations during the active stabilization of RWMs.

2.2. Diagnostics for internal mode-characterization

The main diagnostic used for describing the effects of stable RWMs on the background plasma is the tangential ME-SXR [10–13] presently operating in NSTX. This diagnostic has three

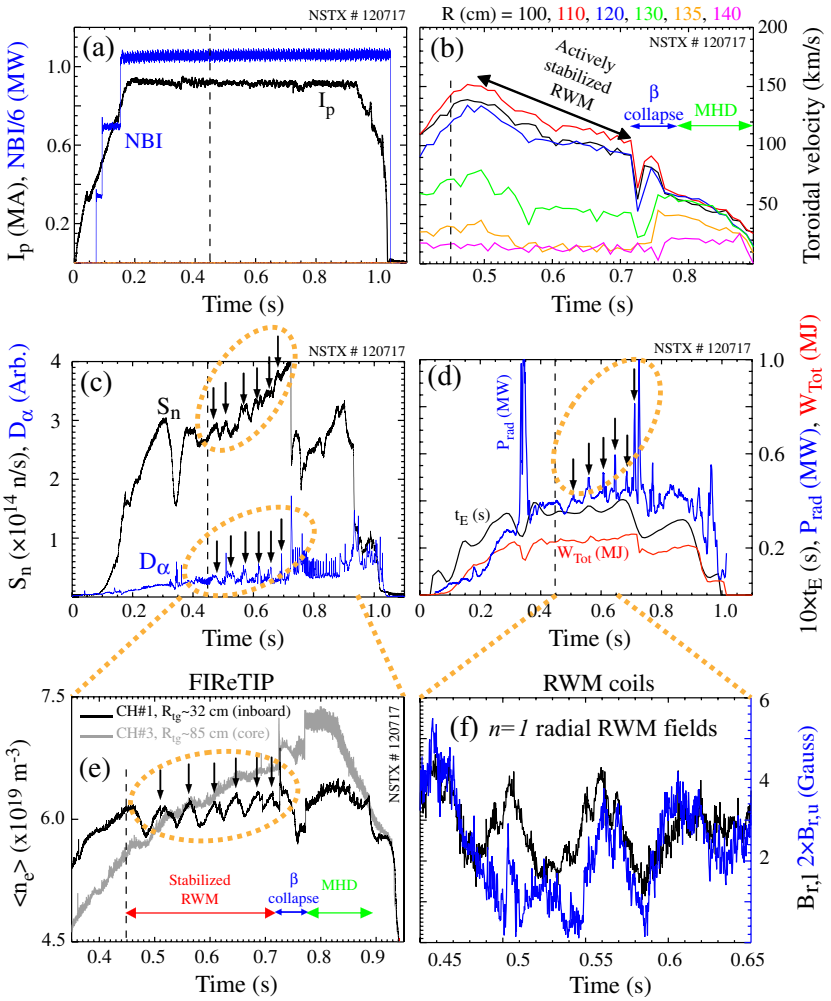

Figure 1. Time histories for (*a*) plasma current and NBI power, (*b*) toroidal rotation velocity during magnetic braking and active stabilization, (*c*) neutron rate and D_α, (*d*) confinement time, radiated power and plasma stored energy, (*e*) FIReTIP measurements at two different tangency radii and (*f*) $n = 1$ radial fields measured by the upper and lower RWM coils.

identical groups of overlapping sightlines that view the same plasma volume using beryllium foils of different thicknesses; the specific selection of these SXR filters was such that their low ($E_{C,10\%} \sim 786$ eV), medium ($E_{C,10\%} \sim 1700$ eV) and high ($E_{C,10\%} \sim 2500$ eV) cut-off energies (for 10% of SXR transmission) are also approximately equal to $1 \times \langle T_e \rangle_l$, $2 \times \langle T_e \rangle_l$ and $3 \times \langle T_e \rangle_l$, where $\langle T_e \rangle_l$ is the line-average electron temperature in typical NSTX discharges. Each group of sightlines views the same plasma volume spanning from the outboard edge to just past the center of the plasma mid-plane (magnetic axis) with a spatial resolution of ~3.5 cm; the diagnostic time resolution is around 50–100 μs. The different temperature sensitivities can be explained by the changes in the measured radiated power ($\mathcal{P}_i$) as shown in equation (1), where $E_{C,i}$ is the cut-off energy for each of the ith filter of choice [12]; for instance, the coefficients affecting the dT_e/T_e term for the low-, medium- and high-energy

emissivities (using an average core plasma temperature of 800 eV and the cut-off energies for 50% transmission) are approximately 1.96, 3.62 and 4.93, respectively. Therefore, the use of a low-energy metallic filter does not contribute much in discriminating whether a perturbation in the SXR emissivity is due to a temperature or a density fluctuation since the coefficients affecting $\mathrm{d}n_\mathrm{e}/n_\mathrm{e}$ and $\mathrm{d}T_\mathrm{e}/T_\mathrm{e}$ terms are of the same order. However, the use of thicker filters and higher cut-off energies will allow the discrimination of temperature over density variations since the term affecting the former can be enhanced by factors of 1.5 to 2.5. The electron temperature measurements can thus be made, both by subtracting the local variations of the energy-sensitive emissivities as indicated in equations (1) and (2) or by computing the ratio of the signals from the high-energy emissivity to that of the low- and medium-energy emissivities using equation (3),

$$\frac{\mathrm{d}\mathcal{P}_i}{\mathcal{P}_i} \approx 2\frac{\mathrm{d}n_\mathrm{e}}{n_\mathrm{e}} + \left(\frac{1}{2} + \frac{E_{C_i}}{T_\mathrm{e}}\right)\frac{\mathrm{d}T_\mathrm{e}}{T_\mathrm{e}} \tag{1}$$

$$\frac{\mathrm{d}\mathcal{P}_j}{\mathcal{P}_j} - \frac{\mathrm{d}\mathcal{P}_i}{\mathcal{P}_i} \approx \left(\frac{\Delta E_{C_{j,i}}}{T_\mathrm{e}}\right)\frac{\mathrm{d}T_\mathrm{e}}{T_\mathrm{e}} \tag{2}$$

$$\frac{\mathcal{P}_j}{\mathcal{P}_i} \approx \exp\left(-\frac{\Delta E_{C_{j,i}}}{T_\mathrm{e}}\right) \tag{3}$$

where $\Delta E_{C_{j,i}} = E_{C_j} - E_{C_i}$ is the cut-off energy difference between the thick and thin filters.

The fast electron temperature measurements shown in this paper are obtained by modeling the slope of the continuum radiation from ratios of the radially inverted emissivity profiles (using equation (3)), with no *a priori* assumptions of plasma density and temperature profiles, magnetic field reconstruction constraints, or need of shot-to-shot reproducibility [11, 12]. The inversion of the SXR emissivity profile is sensitive to the derivative of the measured line-integrated brightness, therefore an appropriate smoothing of the data is generally required for the line-integrated experimental data and its associated noise. The smoothing and inversion procedure is as follows. First, the temporal resolution is reduced with a 1.0 ms averaging window. Then, a cubic spline smoothing procedure was used to process the line-integrated data prior to inversion using a smoothing parameter calculated from the '*rms*' noise of the signal. The degree of smoothing is such that the resultant function fits within the data uncertainty in the averaging window. Lastly, a matrix-based routine is used for Abel-inversion. In this work, the 1D Abel reconstructions of the ~20–25 Hz RWM have been considered only as a *zero*th order approximation of the real 3D reconstructions of the helical non-axisymmetric perturbation. Nonetheless, compared with magnetic measurements, the ME-SXR diagnostic technique has the advantage of providing internal spatial localization applicable to both MHD identification and control.

3. Internal response during stable RWMs and subsequent β_N-collapse

3.1. SXR analysis during stabilized RWM

The ME-SXR emissivity profiles during the time of the active stabilization are shown in figure 2. The edge low-energy emissivity depicted in figure 2(*a*) indicates first that either the $n = 3$ magnetic braking or the $n = 1$ active-stabilizing field may have been responsible for modifying the edge emissivity profiles at early times (see dotted lines within $t \in [450, 500]$ ms). Some of the features characterizing this process are the steepening of the electron density gradient, the intermittent disappearance of the H-mode electron and carbon density ears, as well as the penetration of carbon impurities through the H-mode barrier; the latter is also shown

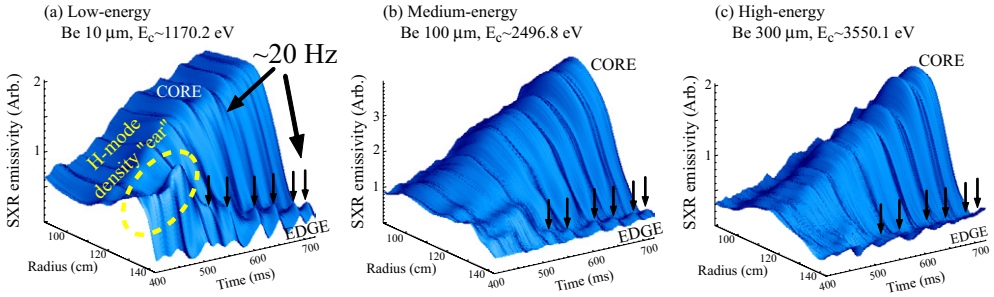

Figure 2. Plots of the three ME-SXR emissivities during the actively RWM control.

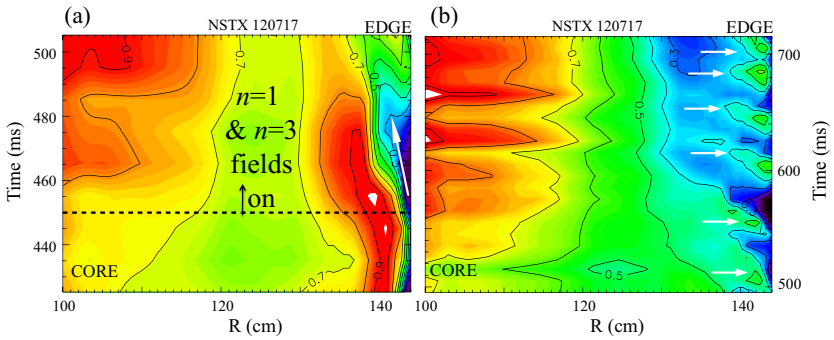

Figure 3. Normalized contour plots of CHERS carbon density (*a*) before and after applying the magnetic braking and active feedback and (*b*) during RWM active stabilization.

in figure 3(*a*) using the charge exchange recombination spectroscopy (CHERS) diagnostic. Whether the intermittent collapse of the density ears is related to crossing a ballooning threshold due to an enhanced plasma pressure or to the change of edge transport as a result of the use of the resonant magnetic perturbations remains to be determined [14]. Second, during the active stabilization of the RWM, the ME-SXR emissivity carries also an edge modulation with the characteristic frequency of ∼20–25 Hz as mentioned above, which in this case can be attributed to an electron and impurity density ($\epsilon_{\mathrm{SXR}} \propto n_{\mathrm{e}} \cdot n_{\mathrm{Z}}$) edge activity (see black arrows in figure 2(*a*) at $R \sim 135$–145 cm, $r/a \sim 0.8$–0.9); these peripheral perturbations seem to also travel radially inward thus modulating the core SXR emission. The normalized carbon density contours shown in figure 3(*b*) indicate also the presence of an edge carbon density modulation with the same frequency as the one observed by the low-energy SXR emissivity; the ion temperature (not shown here) remains constant during the RWM stabilization.

The effects of the stable RWM on the plasma core—assumed originally from the beam-plasma neutron rate modulation shown in figure 1(*c*)—can also be observed in both the 'slow' ∼20–25 Hz modulation of the medium- and high-energy SXR reconstructions shown in figures 2(*b*) and (*c*), as well as in the core carbon density perturbation shown in figure 3(*b*); the latter might have also been responsible for the core beam-plasma neutron rate modulation since in a very first approximation the deuterium density can be expressed as $n_{\mathrm{D}} \approx n_{\mathrm{e}} - Z_{\mathrm{C}} n_{\mathrm{C}}$. The core modulation of the ME-SXR emissivities suggests the presence of an electron temperature perturbation due to their characteristic $\sim \exp\{-E_{\mathrm{C}}/T_{\mathrm{e}}\}$ dependence as discussed above [11, 12]. In fact, the ME-SXR-inferred 'fast' $T_{\mathrm{e}}(R, t)$ measurement during RWM

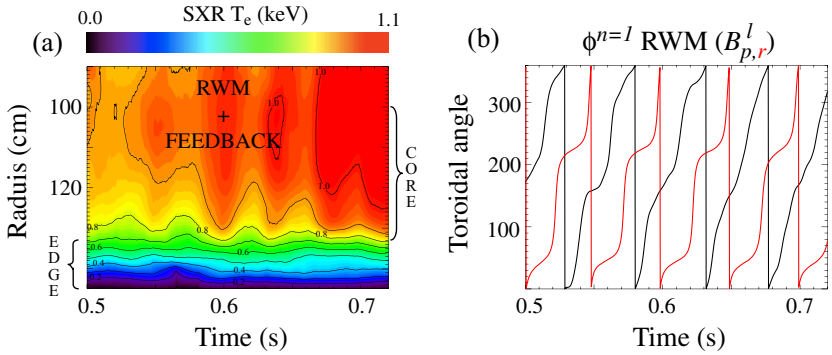

Figure 4. (*a*) Contour plot of the ME-SXR fast $T_e(R, t)$ measurement and (*b*) RWM coil poloidal (black) and radial (red) toroidal phase for the ∼20 Hz $n = 1$ rotating mode.

active-stabilization is shown in figure 4(*a*), and indicates the presence of a 50–100 eV (∼10%) core temperature modulation which is in good agreement with the slow ∼20–25 Hz time history of the rotating $n = 1$ magnetic perturbation measured by the poloidal and radial RWM coils (see figure 4(*b*)). Moreover, this frequency is of the same order as both the inverse wall time ($\tau_w \sim$ 6–7 ms $\Rightarrow f_{wall} \leqslant 1/2\pi\tau_w =$ 22–26 Hz) and the natural resonant field amplification (RFA) 20–30 Hz resonance reported in [6]. The time history of the monotonic safety factor radial profile (not shown here) during RWM stabilization was nearly constant with $q_{min} \approx q_0 = 1.3$ and $q_{95} \sim 10$. In summary, these edge and core density and temperature fluctuations could indicate either the presence of a stabilized (not growing) global mode that is not only confined to the wall but has a radial extent reaching the magnetic axis or a significant displacement of the original wall-mode during the feedback process which will be in tension with the basic assumption of '*mode rigidity*' by which the RWM is confined to the reactor wall; both interpretations are currently under study.

Resolving which mechanism contributes the most to the RWM passive stabilization is still an unsolved problem. For instance, the resonance between the mode and the precession drift frequency of trapped thermal or energetic ions can lead to a significant improvement of the RWM stability limits [16]; a preliminary study on the stabilization of the RWM due to fast ions can be found in [17]. To improve our diagnostic capabilities over the wall Mirnov coils and the tangential ME-SXR array measurements, we have also used a high-throughput SXR diode array in a poloidal multi-energy configuration [18]. Low-amplitude (<1%) MHD activity with mode frequencies ranging from 12 to 18 kHz was found using both magnetic and SXR diagnostics approximately 5 ms before the edge RWM activity (see figure 5). Preliminary calculations at different ion energies and pitch angles indicate that the precession drift frequencies of energetic ions are indeed of the order of 10–20 kHz, and that the mechanism of kinetic stabilization of RWMs by energetic ions could have played an important role in the stability of these H-mode discharges [17, 19, 20].

3.2. Reconstructions during the β_N collapse

By the end of this stabilized period, the plasma experiences a fast β_N-collapse as a result of the high plasma pressure ($\beta_N \sim 5.5$) as is shown in figure 1. This pressure-driven instability is a common non-disruptive MHD feature in high-field tokamaks as well as in NSTX [3], and is characterized by a large-amplitude partial relaxation of the plasma pressure profile. These types of events have also been associated with the growth of a slowly rotating RWM [22],

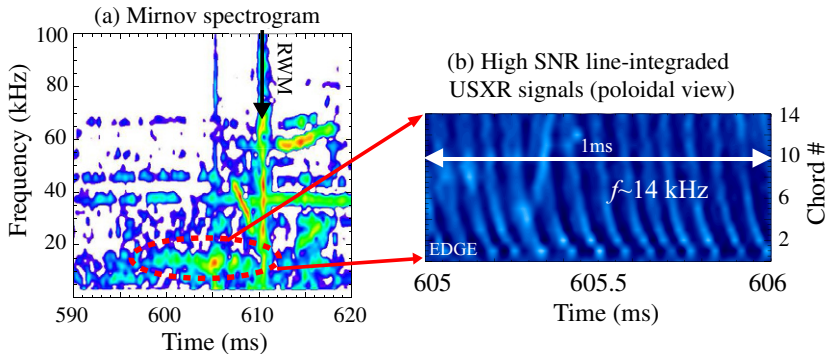

Figure 5. (*a*) Mirnov spectrogram and (*b*) contour plot of SXR brightness before RWM.

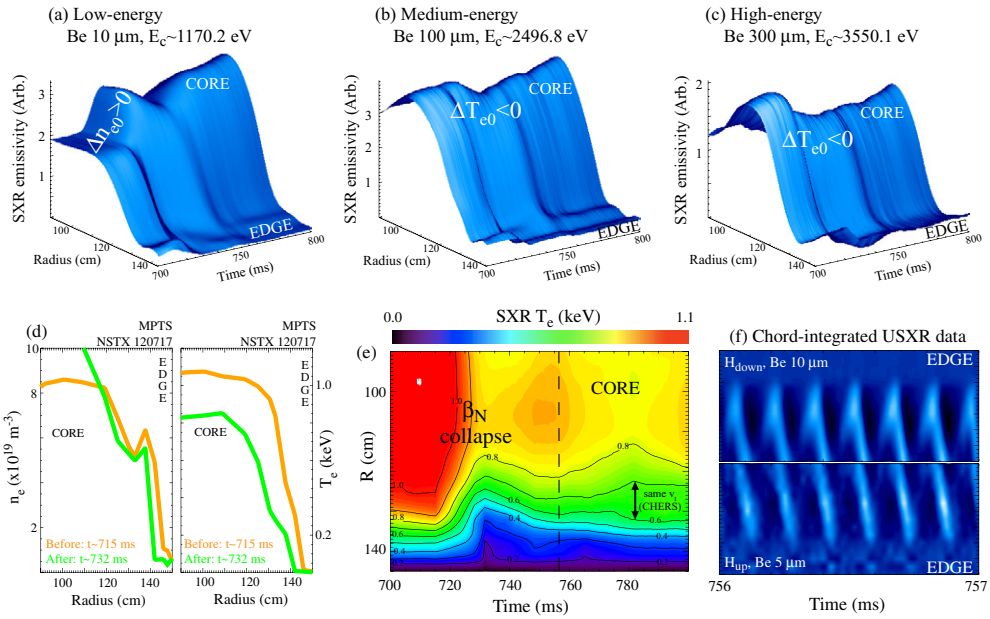

Figure 6. (*a*), (*b*), (*c*) Plots of the three ME-SXR emissivities, (*d*) the intermittent density and temperature data from multi-point Thomson scattering before and after the β_N-collapse, (*e*) the ME-SXR-inferred fast $T_e(R, t)$ measurement and (*f*) the ME-poloidal USXR contours indicating the $(m, n) = (1, 1)$ mode after the β_N-collapse.

which can stop the plasma rotation and cause a fast collapse after the mode amplitude reaches a critical value. The use of the ME-SXR diagnostic can also contribute to the understanding of the modification of the plasma profiles due to its adequate (sub-millisecond) time response. The space and time-resolved SXR emissivities for the β_N-collapse are shown in figure 6. The low-energy SXR emissivity increases substantially in the core (see figure 6(*a*)) in agreement with the sudden increase in the core electron density as shown by both FIReTIP (see figure 1(*e*)) and the intermittent MPTS diagnostics depicted in figure 6(*d*) before and after the collapse. The medium- and high-energy emissivities indicate a peripheral, mid-radius and core T_e 'crash' as well as the inward shift of the plasma center as suggested also by the LRDFIT code [23] (not shown here); the latter is a free boundary equilibrium reconstruction code which includes

temperature iso-surfaces as well as toroidal rotation. The SXR-inferred fast T_e profiles depicted in figure 6(*e*) are broad from the core to mid-radius before the β_N-collapse, but become slightly peaked after it; the temperature drops at the core and mid-radius were of the order of ∼200 eV and in excess of 500 eV, respectively. The LRDFIT reconstruction routine also computes a reduction of β_t and β_N of the order of ∼40%, while the stored energy is reduced from 250 to 150 kJ. The triggering of these pressure-collapses is generally attributed to the growth of a single mode, the mode coupling of different MHD modes and/or the stochastization of magnetic field lines; we estimate that the reason for the failure of the RWM active feedback is related to the strong growth of a ∼40 kHz $n = 2$ mode, several tens of milliseconds before the β_N-collapse at 716 ms. The $n = 2$ mode disappears after the collapse took place giving rise (after few tens of milliseconds) to a $(m, n) = (1, 1)$ mode that is identified by the ∼7 kHz fluctuation in the poloidal SXR array data shown in figure 6(*f*).

4. Summary

A multi-energy soft x-ray (ME-SXR) array is being used for the characterization of resistive wall modes in the NSTX spherical tokamak; compared with magnetic measurements, the ME-SXR diagnostic technique has the advantage of providing internal spatial localization applicable to both MHD identification and control. This compact design can allow the installation of multiple toroidally displaced arrays, important for MHD mode identification and non-magnetic control of fusion plasmas. Present observations with the ME-SXR array indicate the existence of a stable ∼20–25 Hz $n = 1$ RWM; this frequency is also near the natural resonant field amplification (RFA) resonance and inversely proportional to the wall time ($\tau_w \sim$ 6–7 ms $\Rightarrow$ $f_{wall} \leqslant 1/2\pi\tau_w =$ 22-26 Hz). In addition, the stable RWM carries an edge and core density perturbation as well as an electron temperature modulation that also appears to be affecting the plasma core ($r/a \leqslant 0.6$). The amplitude of the latter is of the order of 50–100 eV (∼10%), and its time history is in good agreement with the slow evolution of the $n = 1$ RWM signatures. It has also been pointed out that an energetic particle effect stabilizing the RWM could have also played an important role in these H-mode plasmas [14, 19]. The ME-SXR measurements suggest, in good agreement with the magnetics, that the stabilization of the resistive wall mode in NSTX is not strictly restricted to the reactor wall and edge, and that acting with the stabilizing coils on its global structure may result in density and temperature fluctuations that can be taken into account when designing the feedback process. This multi-energy SXR treatment has also enabled the determination of significant density and temperature variations associated with the β_N-collapse in NSTX.

5. Future work

The implications of this work are important because they indicate the existence of density and temperature perturbations with the same ∼20–25 Hz frequency as the stable $n = 1$ RWM. It is therefore paramount for the operation of future devices to conclude whether an unstable RWM grows from the stable RFA or from another $n = 1$ mode, denoting multi-mode behavior [14]. Some of the new research themes that will help elucidate the physics mechanisms behind the observations raised in this paper have already been included in the last 2009–2010 NSTX experimental campaigns; such topics are for instance (*a*) the development of a synthetic diagnostic capability to perform a detailed comparison between the spectroscopic observations and a mode structure given by theoretical predictions, (*b*) the modification of the plasma density and temperature profiles by the use of the ($n = 3$ braking and the $n = 1$ active feedback) external fields, (*c*) the role of the resonant field amplification and the plasma

response near the marginal stability ($\beta_N \geqslant 5$) and (d) the study of the plasma profiles during the interaction of fast-MHD (e.g. fishbones) with RWMs; the latter is of relevance for determining the effects of energetic ions in stabilizing or destabilizing the RWMs. Future diagnostic studies will also include the use of a second—toroidally displaced—ME-SXR array for $n = 1$ mode identification and control, as well as SXR forward modeling of both unstable and stable RWMs; such modeling will consider mode recognition techniques on the basis of a 3D fit of the tangentially line-integrated data with specific poloidal and toroidal Fourier (m, n) components (e.g. $\mathcal{E} = \mathcal{E}_0 + \tilde{\mathcal{E}}$, where $\mathcal{E}_0$ and $\tilde{\mathcal{E}}$ are the unperturbed and non-axisymmetric perturbation). The temporally fluctuating SXR emissivity can be assumed to arise from a toroidally localized perturbation like $\tilde{\mathcal{E}}(R, \phi, t) = \mathcal{E}_1 \exp\{-(R - R_p)^2/\sigma_R^2\} \exp\{-(\phi - \phi_p(t))^2/\sigma_\phi^2\}$; as the mode rotates, the toroidal angle $\phi_p(t) = \phi_0 + 2\pi f_\phi t$ varies linearly in time with 'f_ϕ', being for instance, the RWM toroidal rotation frequency. More realistic simulations will also be performed using the radial and poloidal eigenfuntions of the toroidal modes.

Acknowledgments

This work was supported by the United States DoE grant No DE-FG02-99ER5452 and DE-FG02-99ER54523 at The Johns Hopkins University, and PPPL DoE contract No DE-AC02-76CH03073 and DE-AC02-09CH11466.

References

[1] Bondeson A and Ward D J 1994 *Phys. Rev. Lett.* **72** 2709
[2] Reimerdes H *et al* 2005 *Nucl. Fusion* **45** 368
[3] Sabbagh S A *et al* 2004 *Nucl. Fusion* **44** 560
[4] Sabbagh S A *et al* 2006 *Nucl. Fusion* **46** 635
[5] Sabbagh S A *et al* 2006 *Phys. Rev. Lett.* **97** 045004
[6] Sontag A C *et al* 2007 *Nucl. Fusion* **47** 1005
[7] Ono M *et al* 2000 *Nucl. Fusion* **40** 557
[8] Delgado-Aparicio L *et al* 2008 *Proc. 50th Annual Meeting of the American Physical Society—APS-DPP (17–21 November 2008)* vol 53, No 14
Delgado-Aparicio L *et al* 2010 *Proc. 51th Annual Meeting of the American Physical Society—APS-DPP (2–6 November 2009)* vol 54, No 15
[9] Delgado-Aparicio L *et al* 2009 *Proc. 36th EPS Conf. on Plasma Physics (Sofia, Bulgaria, 29 June–3 July 2009)* ECA vol 33E P-2.173
[10] Delgado-Aparicio L *et al* 2007 *Appl. Opt.* **46** 6069
[11] Delgado-Aparicio L *et al* 2007 *J. Appl. Phys.* **102** 073304
[12] Delgado-Aparicio L *et al* 2007 *Plasma Phys. Control. Fusion* **49** 1245
[13] Delgado-Aparicio L *et al* 2009 *Nucl. Fusion* **49** 085028
[14] Manickam J, Sabbagh S A and Berkery J 2009 private communication
[15] Lee K C *et al* 2004 *Rev. Sci. Instrum.* **75** 3433
[16] Hu B *et al* 2004 *Phys. Rev. Lett.* **93** 105002
[17] Matsunaga G *et al* 2008 *Proc. 22nd IEAE Fusion Energy Conference (Geneva)* EX/P9-5
Matsunaga G *et al* 2009 *Phys. Rev. Lett.* **103** 045001
[18] Stutman D *et al* 2003 *Rev. Sci. Instrum.* **74** 1982
[19] Berkery J W *et al* 2010 *Phys. Rev. Lett.* **104** 035003
[20] Berkery J W *et al* 2009 *Proc. 51th Annual Meeting of the American Physical Society—APS-DPP (2–6 November 2009)* vol 54, No 15
Berkery J W *et al* 2010 *Phys. Plasmas* **17** 082504
[21] Sabbagh S A *et al* 2009 *Proc. 51th Annual Meeting of the American Physical Society—APS-DPP (2–6 November 2009)* vol 54, No 15
Sabbagh S A *et al* 2010 *Nucl. Fusion* **50** 025020
[22] Strait E J *et al* 2003 *Nucl. Fusion* **43** 430
[23] Menard J *et al* 2006 *Phys. Rev. Lett.* **97** 095002 See also, http://w3.pppl.gov/~jmenard/software/lrdfit/lrdfit-index.html